

# SEIS: SUBSPACE-BASED EQUIVARIANCE AND INVARIANCE SCORES FOR NEURAL REPRESENTATIONS

Huahua Lin, Katayoun Farrahi, and Xiaohao Cai

School of Electronics and Computer Science, University of Southampton, Southampton, UK

## ABSTRACT

Understanding how neural representations respond to geometric transformations is essential for evaluating whether learned features preserve meaningful spatial structure. Existing approaches primarily assess robustness by comparing model outputs under transformed inputs, offering limited insight into how geometric information is organized within internal representations and failing to distinguish between information loss and re-encoding. In this work, we introduce SEIS (*Subspace-based Equivariance and Invariance Scores*), a subspace metric for analyzing layer-wise feature representations under geometric transformations, disentangling equivariance from invariance without requiring labels or explicit knowledge of the transformation. Synthetic validation confirms that SEIS correctly recovers known transformations. Applied to trained classification networks, SEIS reveals a transition from equivariance in early layers to invariance in deeper layers, and that data augmentation increases invariance while preserving equivariance. We further show that multi-task learning induces synergistic gains in both properties at the shared encoder, and skip connections restore equivariance lost during decoding.

**Index Terms**— Equivariance, invariance, representation learning, subspace similarity, deep neural networks

## 1. INTRODUCTION

The remarkable success of deep learning across computer vision, physics simulation, and molecular biology is largely attributed to the effective utilization of inductive biases [1]. Convolutional Neural Networks (CNNs) integrate translation equivariance to handle spatial data efficiently [2], while recent advances in Group equivariant CNNs (G-CNNs) [3] and Graph Neural Networks (GNNs) [4] extend these principles to rotation, reflection, and permutation symmetries. However, despite these architectural guarantees, the empirical behavior of learned representations often diverges from mathematical ideals due to non-linearities, pooling, and discretization artifacts [5]. As a result, downstream performance alone provides an incomplete picture: a model may perform well while internally violating the geometric assumptions it was designed to respect.

The central challenge lies in quantifying these internal properties. Existing approaches [6, 7, 8, 9] typically evaluate whether model outputs remain stable under geometric transformations of the input. However, they require predefining specific target properties (e.g., translation equivariant) to evaluate. Moreover, such tests conflate two distinct failure modes: they cannot distinguish between representations that have lost geometric information entirely (functional failure) and those that preserve the information but re-encode it in a different basis (structural misalignment).

Representational similarity analysis compares neural representations directly without requiring predefined target properties. Canonical Correlation Analysis (CCA) and its variants, including Singular Vector CCA (SVCCA) [10] and Centered Kernel Alignment (CKA) [11], are widely used to quantify similarity between neural layers by measuring correlations between their dominant subspaces across datasets or training stages. However, these tools are exclusively applied to cross-model or cross-layer comparisons, rather than analyzing the stability of a single representation under geometric transformation.

In this work, we address this gap by proposing a novel subspace-based metric/method *Subspace-based Equivariance and Invariance Scores (SEIS)* for analyzing how spatial structure is preserved under transformation by adapting SVCCA with a spatially aware matricization strategy. This approach allows us to explicitly disentangle two properties: *equivariance*, defined as the preservation of information up to a linear transformation, and *invariance*, defined as alignment of the spatial feature basis itself. This distinction enables us to identify when geometric information is preserved but re-encoded, a regime that is invisible to existing metrics.

Our main contributions and findings are as follows:

- We introduce SEIS, the first subspace-based framework to explicitly disentangle equivariance from invariance within internal representations. By introducing a spatially-aware matricization strategy, SEIS enables layer-wise, label-free diagnosis of geometric stability without explicit transformation modeling.
- We reveal the internal geometric trajectory of ResNets, showing that early layers establish strict equivariance, which trades off for invariance in deeper layers. We fur-

ther demonstrate that data augmentation significantly amplifies this deep-layer invariance while preserving the equivariance.

- We demonstrate that the equivariance-invariance trade-off is malleable and dictated by task priors and feature propagation strategies. Multi-task learning reveals a synergistic effect of complementary objectives on shared encoder representations, while skip connections actively restore equivariance lost during decoding

## 2. RELATED WORK

Quantifying the response of neural networks to geometric transformations is crucial for evaluating whether learned representations behave in a structured manner. Although specialized architectures such as G-CNNs [3] theoretically enforce equivariance, empirical measurement remains essential, as these guarantees often degrade in practice due to discretization effects on finite grids [5] and mismatched symmetry assumptions, where imposed priors fail to align with the true data manifold [12].

**Prediction Stability.** A common approach to measuring invariance is quantifying the stability of the final model predictions under input transformations. Metrics such as Accuracy Drop [5] and Relative Corruption Errors [13] measure performance degradation under geometric shifts. To reduce dependence on ground-truth labels, Deng et al. [14] proposed Effective Invariance, which weighs stability by prediction confidence. Additionally, Softmax G-Empirical Equivariance Deviation (G-EED) [7] assesses global deviations using the Kullback–Leibler divergence between predictions and the group orbit average. While these methods provide an intuitive gauge of model invariance, they operate solely at the output level and treat the internal feature extraction as a black box. As a result, they cannot distinguish whether stability arises from robust semantic representations or shortcut learning via spurious correlations [15].

**Element-Wise Feature Statistics.** To probe internal representations, significant effort has been directed toward analyzing the statistics of individual neurons or channels. Prior work has introduced statistical measures that compare a single neuron’s response stability against its global firing profile [6, 9]. More recently, equivariance has been quantified by computing cosine similarity and Pearson correlation between transformed channel activations and the channel activations of transformed inputs [7, 8]. These methods typically aggregate scores by averaging across neurons or channels, implicitly assuming that units operate independently. However, deep neural networks rely on distributed representations where geometric information is encoded in the joint activation space rather than any single direction [11].

**Latent Transformation Modeling.** A more rigorous line of work seeks to model how transformations act within latent

**Table 1:** Comparison of representative approaches for measuring equivariance and invariance. Our method SEIS supports layer-wise analysis, disentangles equivariance from invariance, and operates on joint representations without requiring explicit transformation priors.

Method Category	Layer-wise	Disentangles Eq. & Inv.	Requires $T$	Joint Encoding
Prediction stability	✗	✗	✓	✗
Element-wise feature statistics	✓	✗	✓	✗
Latent transformation modeling	✓	✓	✓	✓
Representation similarity	✓	✗	✗	✓
<b>SEIS (Ours)</b>	✓	✓	✗	✓

representations. Lenc et al. [16] formulated equivariance as a post-hoc regression problem, learning a linear operator that maps representations of original inputs to those of transformed inputs. Architectures such as Spatial Transformer Networks [17] and Capsule Networks [18] share this idea by modeling latent transformations internally for task-driven inference. While expressive, regression-based approaches are computationally expensive, typically requiring supervised optimization and separate regressors for each layer and transformation. For continuous symmetries, the Local Equivariance Error (LEE) avoids explicit regression by measuring infinitesimal equivariance via Lie derivatives [19], but is limited to differentiable transformations with known generators and captures only local, first-order behavior.

**Representation Similarity.** Subspace-based methods have been widely used to compare neural representations across models and layers by analyzing the eigenvectors or singular values of covariance or Gram matrices. CCA and its variants, including SVCCA [10] and CKA [11], capture similarity up to invertible linear transformations, while Procrustes alignment [20] enforces orthogonal correspondence. These methods have not been used to directly assess equivariance or invariance within a representation under input transformations. They treat spatial locations as independent samples when constructing similarity measures, thereby discarding the underlying grid structure. However, their reliance on intrinsic subspace structure rather than explicit transformation priors suggests that they could, in principle, be adapted to analyze geometric stability even when the form of the transformation is unknown.

## 3. METHOD

**Rationale.** While the theoretical definition of equivariance permits arbitrary non-linear transformations, spatial transformations on grid-structured data act as linear operators on the feature space. Furthermore, modern architectures process these features via linear convolutions and element-wise non-linearities that preserve local topology. Consequently, valid geometric representations must remain linearly recoverable under transformation, making subspace analysis a rigorous,

rather than merely heuristic, measure of geometric stability. Building on this insight, we introduce SEIS (equivariance and invariance scores  $S_{\text{equiv}}$  and  $S_{\text{inv}}$  in Section 3.4), a subspace-based metric to diagnose how geometric information is preserved within neural representations under transformations, distinct from existing measures summarized in Table 1.

### 3.1. Notions of Equivariance and Invariance

Let  $f(\cdot)$  denote a fixed neural network layer. Given an input  $x$  and its transformed counterpart  $T(x)$ , we denote the layer activations as  $f(x)$  and  $f(T(x))$ , respectively. We formalize two notions of geometric consistency.

**Equivariance.** A representation is equivariant if the information encoded in  $f(x)$  is preserved in  $f(T(x))$  up to a linear change of basis. Formally, equivariance holds if there exists a linear operator  $M$  such that  $f(T(x)) \approx Mf(x)$ . This implies functional preservation of information, allowing features to be redistributed (e.g., permuted) while remaining linearly recoverable.

**Invariance.** Invariance imposes a stronger constraint: the feature basis itself must remain aligned. This implies that the mapping  $M$  is approximately the identity (up to sign or permutation), i.e.,  $f(T(x)) \approx f(x)$ . This reflects robustness at the level of feature organization, where the representation responds consistently without requiring a change of basis.

### 3.2. Spatially-Aware Matricization

Let  $\mathbf{Z} \in \mathbb{R}^{b \times c \times h \times w}$  denote the activation tensor for a batch of inputs, where  $b$ ,  $c$ ,  $h$ , and  $w$  correspond to batch size, channel count, and spatial dimensions. Given a spatial transformation  $T$  applied to the input  $x$ , we obtain paired activations  $\mathbf{Z} = f(x)$  and  $\mathbf{Z}' = f(T(x))$ .

Unlike standard representational similarity (e.g., CCA and CKA), which flatten spatial dimensions into the sample axis and compare channel-wise feature subspaces, SEIS treats spatial locations as features and aggregates channel responses across samples as observations. Specifically, we reshape the activations into matrices  $\mathbf{A}, \mathbf{A}' \in \mathbb{R}^{d \times n}$ , where  $d = h \cdot w$  indexes spatial coordinates and  $n = b \cdot c$  indexes observations. This inversion allows us to measure the stability of the spatial feature basis itself, rather than the alignment of channel-wise feature subspaces.

Under our representation, a spatial transformation acts as a permutation or interpolation operator on the feature axis. Consequently, linear relationships between  $\mathbf{A}$  and  $\mathbf{A}'$  directly reflect whether spatial information is preserved, redistributed, or destroyed by the transformation.

### 3.3. Subspace Denoising via SVD

Neural representations are typically high-dimensional and may contain substantial redundancy or noise, including inactive or weakly informative neurons. To focus the analysis on

informative signal, we perform Singular Value Decomposition (SVD) on each matrix,

$$\mathbf{A} = \mathbf{U}_A \boldsymbol{\Sigma}_A \mathbf{V}_A^\top, \quad \mathbf{A}' = \mathbf{U}_{A'} \boldsymbol{\Sigma}_{A'} \mathbf{V}_{A'}^\top. \quad (1)$$

We retain the leading  $k_A$  and  $k_{A'}$  left singular vectors  $\tilde{\mathbf{U}}_A \in \mathbb{R}^{d \times k_A}$  and  $\tilde{\mathbf{U}}_{A'} \in \mathbb{R}^{d \times k_{A'}}$  that explain 99% of the cumulative variance, yielding denoised subspace representations

$$\tilde{\mathbf{A}} = \tilde{\mathbf{U}}_A^\top \mathbf{A} \in \mathbb{R}^{k_A \times n}, \quad \tilde{\mathbf{A}}' = \tilde{\mathbf{U}}_{A'}^\top \mathbf{A}' \in \mathbb{R}^{k_{A'} \times n}. \quad (2)$$

This step is critical for numerical stability, as applying CCA directly to high-dimensional activations often leads to ill-conditioned covariance estimates and non-convergent eigenvalue decompositions.

### 3.4. Quantifying Equivariance and Invariance

We apply CCA to the denoised subspaces  $\tilde{\mathbf{A}}$  and  $\tilde{\mathbf{A}}'$ . CCA identifies pairs of projection vectors  $\mathbf{w}_i \in \mathbb{R}^{k_A}$  and  $\mathbf{v}_i \in \mathbb{R}^{k_{A'}}$  that maximize the correlation between projected variates

$$\mathbf{p}_i = \mathbf{w}_i^\top \tilde{\mathbf{A}} \in \mathbb{R}^n, \quad \mathbf{q}_i = \mathbf{v}_i^\top \tilde{\mathbf{A}}' \in \mathbb{R}^n, \quad i = 1, \dots, r, \quad (3)$$

where  $r = \min(k_A, k_{A'})$ . These canonical components capture directions of maximal shared information between the original and transformed representations.

**Equivariance Score.** Functional equivariance requires that information to be preserved under transformation up to a linear change of basis. We quantify this by mean absolute cosine similarity between the canonical variates

$$S_{\text{equiv}} = \frac{1}{r} \sum_{i=1}^r \left| \frac{\langle \mathbf{p}_i, \mathbf{q}_i \rangle}{\|\mathbf{p}_i\|_2 \|\mathbf{q}_i\|_2} \right|. \quad (4)$$

Since canonical variates  $\mathbf{p}_i$  and  $\mathbf{q}_i$  are centered, this quantity is equivalent to the mean canonical correlation. A high  $S_{\text{equiv}}$  indicates that spatial information is preserved in the representation, even if redistributed across feature dimensions, consistent with linear equivariance.

**Invariance Score.** Invariance imposes a stronger requirement: not only must information be preserved, but the spatial feature basis itself should remain aligned. To capture this, we measure the cosine similarity between the corresponding CCA projection vectors,

$$S_{\text{inv}} = \frac{1}{r} \sum_{i=1}^r \rho_i \cdot \left| \frac{\langle \mathbf{w}_i, \mathbf{v}_i \rangle}{\|\mathbf{w}_i\|_2 \|\mathbf{v}_i\|_2} \right|, \quad (5)$$

where  $\rho_i$  denotes the  $i$ -th canonical correlation coefficient. Weighting by  $\rho_i$  suppresses directions that carry little shared information and ensures that alignment is assessed only where equivariance is meaningful. A high  $S_{\text{inv}}$  indicates that the features are not only recoverable but are spatially aligned, reflecting robustness to the transformation.

## 4. EXPERIMENTS

### 4.1. Validation on Synthetic Transformations

**Experimental Setup.** We validate SEIS using a controlled synthetic setup that isolates geometric effects from training dynamics. Activations are extracted from a single convolutional layer on MNIST, and paired representations are constructed by directly applying spatial transformations to the reference activations. This yields two ground-truth regimes: *perfect invariance*, where the representation is unchanged, and *strict equivariance*, where spatial transformations act linearly on the representation. This setting allows us to directly verify whether SEIS recovers known geometric relationships.

We evaluate six conditions: an identity control, four geometric transformations (translation, scaling, rotation, and a composite affine transform), and a random baseline. Transformation parameters are sampled stochastically: translation is limited to  $\pm 15\%$  of the spatial dimension; scaling factors range from 0.8 to 1.2; rotation is sampled from the full range of  $360^\circ$ ; and a composite affine transformation combines all three distortions simultaneously. For each condition, both  $\mathcal{S}_{\text{equiv}}$  and  $\mathcal{S}_{\text{inv}}$  are computed and reported as the mean over 50 independent trials.

**Results.** Figure 1 shows that SEIS reliably distinguishes between controlled regimes. In the identity condition, both scores approach 1.0, confirming the correct calibration of the metrics. Under all geometric transformations, the invariance score drops sharply, indicating that feature responses change with the transformation rather than remaining fixed at the same spatial locations. At the same time, the equivariance score remains high ( $\mathcal{S}_{\text{equiv}} > 0.85$ ), correctly reflecting that the underlying information is preserved and remains linearly recoverable despite spatial redistribution. In contrast, the random baseline yields near-zero scores for both metrics, demonstrating that the high equivariance observed in the previous cases arises from structured geometric transformations rather than from spurious correlations in high-dimensional feature spaces.

### 4.2. Depth-wise Evolution

**Experimental Setup.** We analyze how equivariance and invariance evolve during training by evaluating SEIS on internal representations induced by an input image and its affine transformed counterpart. We train ResNet architectures of varying scales on CIFAR-100 for 200 epochs using SGD with momentum 0.9, weight decay  $5e^{-4}$ , and batch size 128. The initial learning rate is set to 0.1 and decayed by a factor of 0.2 at epochs 60, 120, and 160. We observe qualitatively similar behaviors across all ResNet variants; for brevity, we report results for ResNet-18.

During evaluation, layer activations are computed on a fixed subset of the CIFAR-100 test set for each input image and for a transformed version obtained via a random affine

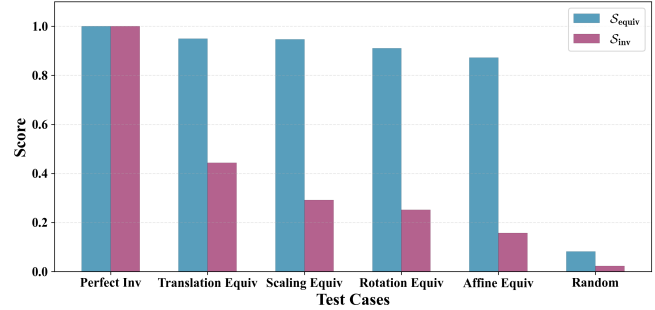


**Fig. 1:** Validation of SEIS on MNIST activations using controlled transformations. The identity case (*left*) yields high scores for both metrics, geometric transformations (*middle*) preserve equivariance but reduce invariance, and the random baseline (*right*) produces negligible scores.

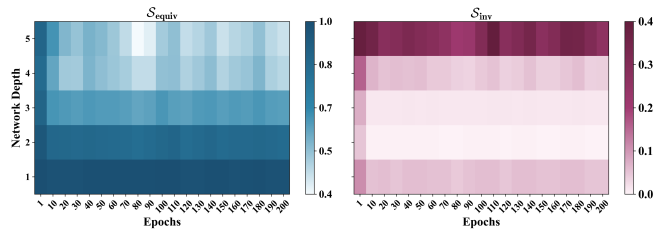


**Fig. 2:** Depth-wise equivariance ( $\mathcal{S}_{\text{equiv}}$ ) (*left panel*) and invariance ( $\mathcal{S}_{\text{inv}}$ ) (*right panel*) scores across training epochs for ResNet-18 on CIFAR-100. Both properties stabilize early and exhibit a clear depth-dependent pattern.

transformation, with rotations in  $[-15^\circ, 15^\circ]$ , translations up to 5% of the image size, and scaling in  $[0.9, 1.1]$ .

**Training Dynamics.** Figure 2 shows the evolution of equivariance and invariance across network depth during standard training. Both scores stabilize within the first 10 epochs, indicating that these properties are established early and remain largely unchanged thereafter. A clear depth-dependent pattern emerges: equivariance is highest in early layers ( $\mathcal{S}_{\text{equiv}} \approx 0.9$ ) and gradually decreases with depth, while invariance exhibits the opposite trend, increasing from low values in shallow layers ( $\mathcal{S}_{\text{inv}} \approx 0.1$ ) to its highest value in the deepest layer ( $\mathcal{S}_{\text{inv}} \approx 0.3$ ). This progression is consistent with the hierarchical organization of classification networks, in which early layers preserve spatial structure and deeper layers develop more transformation-tolerant representations.

**Effect of Data Augmentation.** We next examine the effect of training-time data augmentation by comparing models trained with (using the same family of affine transformations during evaluation) and without affine augmentations. As shown in Figure 3, augmented models maintain higher equivariance in deeper layers ( $\mathcal{S}_{\text{equiv}} \approx 0.6$  versus  $\approx 0.4$  without augmentation), indicating improved preservation of geometric information. At the same time, invariance is consistently strengthened across depth, with the deepest layer reaching  $\mathcal{S}_{\text{inv}} \approx 0.4$  com-

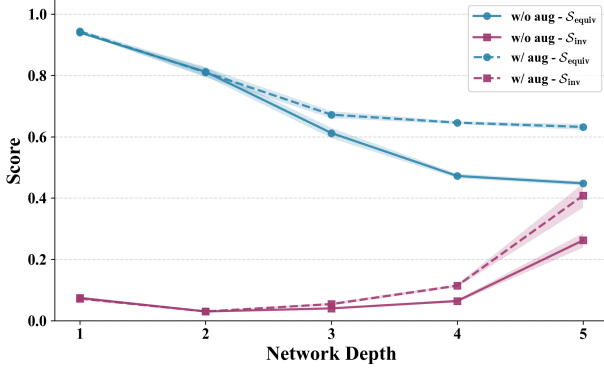


**Fig. 3:** Effect of affine data augmentation on equivariance and invariance across network depth for ResNet-18 on CIFAR-100. Augmentation increases invariance while preserving equivariance in deeper layers.

pared to  $\approx 0.3$  in the non-augmented model. These results indicate that affine augmentation promotes representations that are more transformation-tolerant while preserving equivariant structure, consistent with empirical observations based on Pearson correlation measures [8].

### 4.3. Effects of Task Objectives

Different computer vision tasks impose distinct geometric requirements on learned representations. Semantic segmentation requires precise spatial localization and therefore benefits from equivariance, whereas image classification prioritizes abstraction over spatial transformations and thus benefits from invariance. We investigate whether these task-specific objectives systematically shape the geometric properties encoded in neural representations, and whether Multi-Task Learning (MTL) induces a predictable trade-off between equivariance and invariance in shared encoder layers. In addition, we explicitly compare two decoder designs—Fully Convolutional Network (FCN) and U-Net [21]—to isolate how architectural choices interact with task objectives to influence equivariance propagation.

**Experimental Setup.** We train three types of model on PASCAL VOC 2012: (1) Classification-only using image-level labels, (2) Segmentation-only using pixel-level masks, and (3) MTL with a shared encoder and task-specific decoders. All models employ an identical encoder architecture (ResNet-50 backbone), are optimized using SGD with momentum 0.9, an initial learning rate of 0.1 decayed by a factor of 0.2 at epochs 60 and 120, and are trained for 200 epochs. For MTL, we additionally use a weighted loss  $\mathcal{L}_{\text{seg}} + \lambda \mathcal{L}_{\text{cls}}$  with  $\lambda \in \{0.25, 0.50, 0.75\}$  to examine how task balance modulates the equivariance–invariance trade-off in shared representations. Equivariance and invariance are quantified using SEIS at each network layer under random affine transformations applied to a held-out test set.

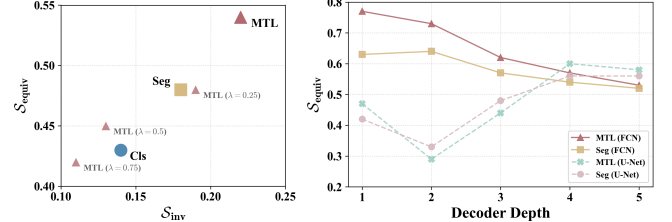


**Fig. 4:** *Left panel:* Equivariance ( $S_{\text{equiv}}$ ) versus invariance ( $S_{\text{inv}}$ ) at the bottleneck layer for Classification (Cls), Segmentation (Seg), and Multi-Task Learning (MTL). *Right panel:* Equivariance trajectories across decoder depth, comparing FCN and U-Net decoders under single-task (Seg) and multi-task objectives.

**Results.** Figure 4 *left* shows that the geometric properties of the bottleneck layer diverge significantly depending on the task objective. Surprisingly, the MTL model ( $\lambda = 1.0$ ) achieves both the highest invariance ( $S_{\text{inv}} = 0.22$ ) and the highest equivariance ( $S_{\text{equiv}} = 0.54$ ) among all models. This supports the hypothesis that complementary objectives act as an inductive bias, encouraging the shared encoder to balance spatial precision with semantic abstraction [22]. In contrast, the classification model exhibits the lowest scores, attributed to global average pooling, which removes the penalty for spatial misalignment. Notably, this synergy is sensitive to task balance; reducing the classification weight  $\lambda$  progressively erodes these structural gains, shifting representations toward single-task regimes.

Figure 4 *right* compares equivariance trajectories across decoder depth, revealing distinct structural strategies. The FCN decoder exhibits a monotonic decay in equivariance, reflecting its reliance on information encoded solely at the bottleneck. Notably, MTL-FCN starts with higher equivariance (0.77) than the single-task segmentation baseline (0.63), indicating MTL enriching the shared encoder representation. In contrast, U-Net decoder displays a non-monotonic equivariance profile, with an initial decline followed by a pronounced recovery in later layers. This behavior confirms skip connections act as a structural bypass, dynamically re-injecting spatial fidelity from early encoder stages and restoring equivariance that would otherwise be lost during decoding.

## 5. CONCLUSIONS

We presented SEIS, a subspace-based metric for dissecting the geometric behavior of neural representations by disentangling equivariance from invariance. Our experiments show that the equivariance–invariance trade-off is not an inherent property of network architecture but is actively shaped by training choices, including augmentation, task objectives, and feature propagation strategies. SEIS provides a necessary lens for ensuring that models intended for geometric tasks respect the symmetries they are assumed to learn and beyond.

## 6. REFERENCES

- [1] Michael M Bronstein, Joan Bruna, Yann LeCun, Arthur Szlam, and Pierre Vandergheynst, “Geometric deep learning: going beyond euclidean data,” *IEEE Signal Processing Magazine*, vol. 34, no. 4, pp. 18–42, 2017.
- [2] Yann LeCun, Bernhard Boser, John S Denker, Donnie Henderson, Richard E Howard, Wayne Hubbard, and Lawrence D Jackel, “Backpropagation applied to handwritten zip code recognition,” *Neural Computation*, vol. 1, no. 4, pp. 541–551, 1989.
- [3] Taco Cohen and Max Welling, “Group equivariant convolutional networks,” in *International conference on machine learning*. PMLR, 2016, pp. 2990–2999.
- [4] Maurice Weiler and Gabriele Cesa, “General E(2)-equivariant steerable CNNs,” *Advances in Neural Information Processing Systems*, vol. 32, 2019.
- [5] Aharon Azulay and Yair Weiss, “Why do deep convolutional networks generalize so poorly to small image transformations?,” *Journal of Machine Learning Research*, vol. 20, no. 184, pp. 1–25, 2019.
- [6] Ian Goodfellow, Honglak Lee, Quoc Le, Andrew Saxe, and Andrew Ng, “Measuring invariances in deep networks,” *Advances in Neural Information Processing Systems*, vol. 22, 2009.
- [7] Henry Kvinge, Tegan Emerson, Grayson Jorgenson, Scott Vasquez, Tim Doster, and Jesse Lew, “In what ways are deep neural networks invariant and how should we measure this?,” in *Advances in Neural Information Processing Systems*, 2022, vol. 35, pp. 32816–32829.
- [8] Robert-Jan Bruintjes, Tomasz Motyka, and Jan van Gemert, “What affects learned equivariance in deep image recognition models?,” in *Proceedings of the IEEE/CVF Conference on Computer Vision and Pattern Recognition*, 2023, pp. 4839–4847.
- [9] Facundo Manuel Quiroga, Jordina Torrents-Barrena, Laura Cristina Lanzarini, and Domenec Puig-Valls, “Invariance measures for neural networks,” *Applied Soft Computing*, vol. 132, pp. 109817, 2023.
- [10] Maithra Raghu, Justin Gilmer, Jason Yosinski, and Jascha Sohl-Dickstein, “Svcca: Singular vector canonical correlation analysis for deep learning dynamics and interpretability,” *Advances in Neural Information Processing Systems*, vol. 30, 2017.
- [11] Simon Kornblith, Mohammad Norouzi, Honglak Lee, and Geoffrey Hinton, “Similarity of neural network representations revisited,” in *International Conference on Machine Learning*. PMLR, 2019, pp. 3519–3529.
- [12] Gregory Benton, Marc Finzi, Pavel Izmailov, and Andrew G Wilson, “Learning invariances in neural networks from training data,” *Advances in Neural Information Processing Systems*, vol. 33, pp. 17605–17616, 2020.
- [13] Dan Hendrycks and Thomas Dietterich, “Benchmarking neural network robustness to common corruptions and perturbations,” *International Conference on Learning Representations*, 2019.
- [14] Weijian Deng, Stephen Gould, and Liang Zheng, “On the strong correlation between model invariance and generalization,” *Advances in Neural Information Processing Systems*, vol. 35, pp. 28052–28067, 2022.
- [15] Robert Geirhos, Jörn-Henrik Jacobsen, Claudio Michaelis, Richard Zemel, Wieland Brendel, Matthias Bethge, and Felix A Wichmann, “Shortcut learning in deep neural networks,” *Nature Machine Intelligence*, vol. 2, no. 11, pp. 665–673, 2020.
- [16] Karel Lenc and Andrea Vedaldi, “Understanding image representations by measuring their equivariance and equivalence,” in *Proceedings of the IEEE Conference on Computer Vision and Pattern Recognition*, 2015, pp. 991–999.
- [17] Max Jaderberg, Karen Simonyan, Andrew Zisserman, et al., “Spatial transformer networks,” *Advances in Neural Information Processing Systems*, vol. 28, 2015.
- [18] Sara Sabour, Nicholas Frosst, and Geoffrey E Hinton, “Dynamic routing between capsules,” *Advances in Neural Information Processing Systems*, vol. 30, 2017.
- [19] Nate Gruver, Marc Finzi, Micah Goldblum, and Andrew Gordon Wilson, “The Lie derivative for measuring learned equivariance,” *International Conference on Learning Representations*, 2022.
- [20] Frances Ding, Jean-Stanislas Denain, and Jacob Steinhardt, “Grounding representation similarity through statistical testing,” *Advances in Neural Information Processing Systems*, vol. 34, pp. 1556–1568, 2021.
- [21] Olaf Ronneberger, Philipp Fischer, and Thomas Brox, “U-net: Convolutional networks for biomedical image segmentation,” in *International Conference on Medical Image Computing and Computer-assisted Intervention*. Springer, 2015, pp. 234–241.
- [22] Simon Vandenhende, Stamatios Georgoulis, Wouter Van Gansbeke, Marc Proesmans, Dengxin Dai, and Luc Van Gool, “Multi-task learning for dense prediction tasks: A survey,” *IEEE Transactions on Pattern Analysis and Machine Intelligence*, vol. 44, no. 7, pp. 3614–3633, 2021.